Supplementary Material to the article
«Localized superconductivity in LaB_6 hexaboride with dynamic charge stripes»

Table S1. Crystallographic characteristics, details of X-ray diffraction experiments with the LaB_6 single crystals.

Sample	LaB_6	
T, K	30	85
Space group, Z	Pm–3m, 1	
Lattice parameter a, Å	4.1510(1)	4.1527(1)
Radiation type; λ, Å	AgK_α, 0.56087	MoK_α; 0.71073
Maximum linear size of the sample, mm	0.078	
Diffractometer	XtaLAB Synergy-DW HyPix Arc 150°	
Scan mode	Ω	
Absorption correction	polyhedron	
Absorption coefficient μ, mm^{-1}; T_{min}, T_{max}	7.67; 0.724, 0.801	14.585; 0.52, 0.701
θ_{max}, deg	45.78	73.89
Limits of h; k; l	$-10 \le h \le 10$; $-10 \le k \le 10$; $-10 \le l \le 10$	$-11 \le h \le 11$; $-11 \le k \le 11$; $-11 \le l \le 11$
Number of reflections: observed; with $I > 3\sigma I$; independent; R_{int}, %	23 084; 9299; 165; 13.88	20 841; 19395; 193; 2.72
Refinement method	Least squares on F	
Numbers of refined parameters	6	
Extinction type	Type 1, Lorentzian	
$R1(\|F\|)$ / $wR2(\|F\|)$, %	1.94 / 2.11	0.82 / 1.23
Goodness of fit, S	1.13	1.12
$\Delta\rho_{min}/\Delta\rho_{max}$, e/Å^3	–1.34 / 1.26	–0.88 / 0.84
Programs	CrysAlis Pro v.43.92, Jana2006	

Table S2. Small JT-induced static distortions of the LaB_6 crystal lattices.

Chemical formula	LaB_6	
T, K	30	85
a, Å	4.1507(1)	4.1533(1)
b, Å	4.1508(1)	4.1519(1)
c, Å	4.1513(1)	4.1528(1)
α, deg	90.003(2)	89.974(2)
β, deg	90.033(2)	90.035(2)
γ, deg	90.015(2)	90.008(2)

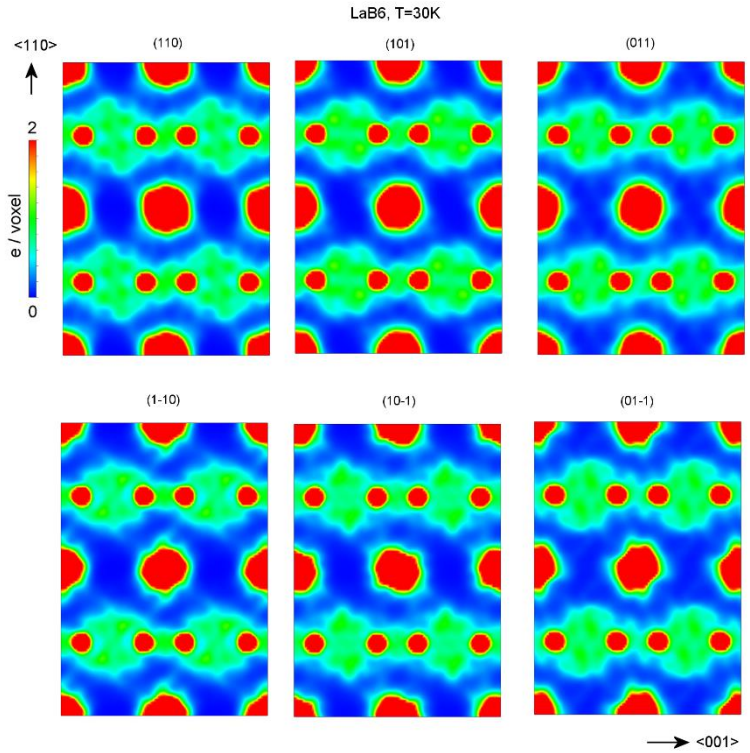

(a)

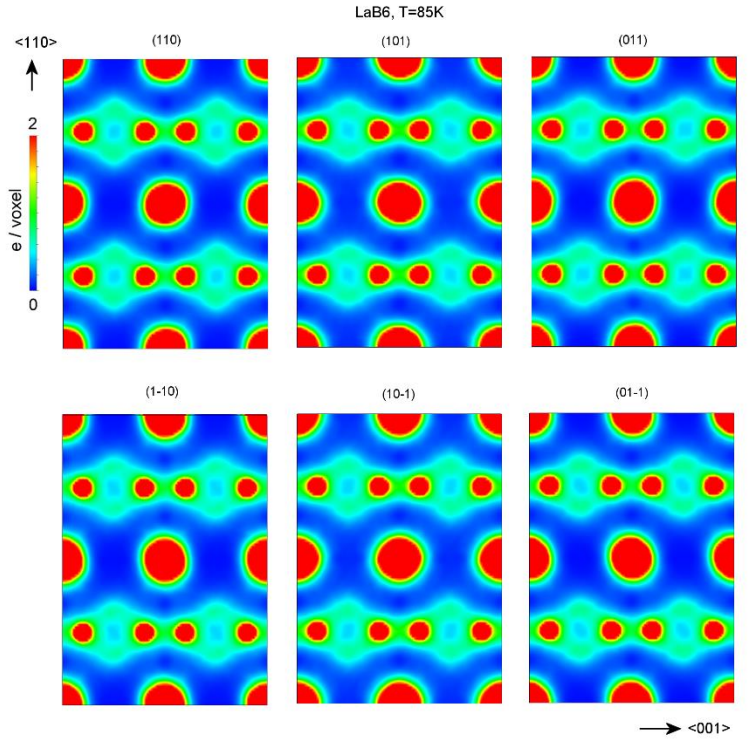

(b)

Fig. S1. MEM maps of LaB_6 in the {110} planes at temperatures of 30 K (a) and 85 K (b). Electron density peaks are cut off at a height of 2 e/voxel to highlight fine details of the electron density (ED) distribution at lattice interstices. Large red circles – La positions; small red circles – positions B. Shades of green highlight the interstitial electron density in the framework of boron atoms.

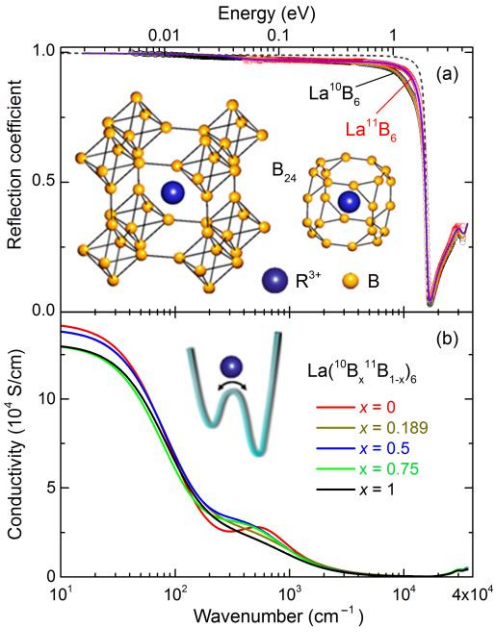

Fig. S2. (a) Reflectivity spectra of $La^{10}B_6$ and $La^{11}B_6$ single crystals (dots). Solid lines show the results of least-square fitting of the spectra with the Drude term and two Lorentzian terms. The dashed line shows the best fit of the reflectivity spectrum of $La^{11}B_6$ obtained by the Drude term (conductivity σ_{DC}^{Drude}=143110 $Ohm^{-1}cm^{-1}$ and relaxation rate γ^{Drude}=260 cm^{-1}). The obtained spectra of the real part of conductivity of all measured $La(^{10}B_x{}^{11}B_{1-x})_6$ crystals are presented in panel (b). The insets in panels present the crystal structure of RB_6 and Fedorov B_{24} polyhedra centered by R^{3+} ion and vibrations of La- ion in the double-well potential (schematically). The data are recorded at T=300 K (see [18] in the manuscript).

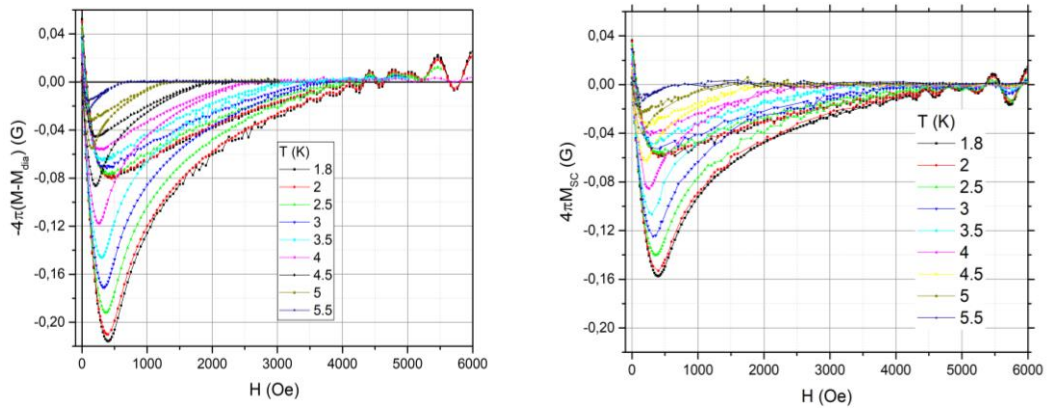

(a) (b)

Рис. S3. Magnetic field dependences of magnetization in the superconducting state of LaB_6 for **H** // [100] direction of the external magnetic field: (a) for a crystal #3 of size 1x2x12 mm^3 and (b) for three crystals of size 1x0.55x12 mm^3 each, prepared from the crystal #3.

The single crystals' growth.

The preparation of lanthanum hexaboride (LaB_6) single crystals consists of several stages, which include the synthesis of LaB_6 in the form of a powder during the borothermal reduction of lanthanum oxide (La_2O_3), the preparation of sintered rods from this powder, and the growing of single crystals from the rods by crucible-less floating-zone (FZ) melting technique in the "Crystal-111" unit with radio-frequency induction heating.

First, the La_2O_3 powder anneals at 800^0C for 2 hours to remove the crystallization water, after which a mixture of oxide and boron is prepared according to the equation for the solid-state reaction of the borothermal reduction:

$$La_2O_3 + 15B \rightarrow 2LaB_6 + 3BO\uparrow \qquad (S1)$$

A small excess of boron (3 wt %) was introduced into the initial charge to compensate for possible losses of boron due to the high pressure of its vapor at the synthesis temperature. The charge was mechanically mixed for several days, sifting through a sieve at least 5 times in order to break conglomerates based on oxide and boron and prepare, as far as possible, a homogeneous mixture. The prepared mixture was pressed into tablets with a diameter of 15 mm and a height of 10 mm, which were kept in a vacuum furnace for an hour at a temperature of 1650^0C. The temperature was raised slowly, at a rate of about 30 deg/min, to ensure the removal of the resulting gases. The equation (S1) reflects the overall reaction (initial (left side) and final (right side) stages), but the reduction reaction itself goes through intermediate stages that include the formation of borate ($LaBO_3$), a trace amount of hexaboride (LaB_6) and free boron (B_{free}) (~1055^0C) and the subsequent reaction of the $LaBO_3$ with the remaining boron to form a hexaboride (1175^0C) [1]

$$La_2O_3 + B \rightarrow LaBO_3 + LaB_6 + B_{free} \qquad (S2),$$

$$LaBO_3 + B_{free} \rightarrow LaB_6 + 3BO\uparrow \qquad (S3).$$

Since the solid-phase synthesis is determined by diffusion processes, an additional homogenization of the synthesized powder was carried out: the sintered tablets were broken, pressed again and kept in vacuum at 1750^0C for an hour. The annealed tablets were broken again; the resulting powder was pressed in the cold into rods with a diameter of 8 mm and a length of 60 mm, which were sintered for an hour at 1750^0C in a vacuum. Final homogenization occurs in the melt during crystal growth.

For LaB_6 preparation we used high purity substances: natural boron (isotope distribution: 18.8% ^{10}B, 81.2% ^{11}B, AVIABOR Inc., Dzerzhinsk, Russia, with purity > 99.9 mass %, the procedure of boron preparation excludes its contamination by carbon) and La_2O_3 from the Federal State Research and Design Institute of Rare Metal Industry (Moscow, Russia) with purity of 99.997 mass %.

The synthesis, annealing of tablets and sintering of the rods took place in the same ZrB_2 crucibles. The melting temperature of ZrB_2 is ~ 3000^0C; therefore, contamination with crucible material is excluded. However, the original sintered rods may be contaminated with iron due to intermediate grinding of the synthesized and sintered tablets in the Abikha steel mortar, but this element is effectively purified during the zone melting process [2-4]. Thus, the initial LaB_6 rods for crystal growth were identical in composition and purity.

FZ melting is carried out in a closed chamber under the pressure of high-purity argon (volume fraction of argon is not less than 99.993 %). The process of the chamber preparing for melting is also identical for all crystals. Preliminarily the chamber is pumped out to 10^{-3} mm Hg (0.1333 Pa), then it is filled with argon up to 0.2 MPa and pumped out again, after which it is filled with argon to a predetermined pressure, and the melting process begins.

The main technological parameters that determine the growth of high-quality LaB_6 single crystals (growth rate, feed and rotation speed of the seed, Ar pressure in the chamber, etc.) are summarized in the Table S3. All crystals were grown in a single pass of the melting zone, with single-crystalline seeds with

either a random orientation or a specified orientation, their dimensions being 5-6 mm in diameter and up to 80 mm in length. The most important parameter is the crystallization rate or crystal growth rate; for all crystals the rate has been equal to 0.55 mm/min. The feed rate of the sintered rods is less than the crystal growth rate and varies slightly due to small differences in the mass of the feed rods and the need to maintain a constant diameter of the molten zone. The growing crystals did not rotate at all. The rotation speed of the feed rods is slightly different, and it is adjusted during growth; a necessary condition is to maintain a constant shape of the zone.

Table S3. Summary of the technological parameters for growing LaB_6 single crystals used to obtain the samples studied.

Crystal number	Seed position	Crystal growth rate (mm/min)	Feed rod rate (mm/min)	Seed/Feed rod rotation rate (rpm)	Ar pressure (MPa)	Remarks
# 1	lower shaft	0.55	0.50	0/8	0.1	
# 2	lower shaft	0.55	0.50	0/8	0.1	
# 3	upper shaft	0.55	0.45	0/6	0.1	
# 4	upper shaft	0.55	0.45	0/11	0.1	
# 5	upper shaft	0.55	0.40	0/15	0.3	Argon-gas additional purification

In the case of crystal # 5, additional purification of argon from possible impurities of other gases was carried out directly in the growth chamber by using Ti as a getter. No matter how sealed the chamber is, the presence of impurity gases cannot be unambiguously excluded due to their partial pressures. Oxygen is especially undesirable because it promotes the growth of block crystals. This additional operation made it possible to grow crystal # 5 with the best residual resistivity ratio RRR>150. In addition, we used the highest rotation rate of the feed rod for this crystal compared to other crystals, which contributed to a more uniform temperature distribution in the melt zone and alignment of the crystallization front, reducing thermal and mechanical stresses in the crystal.

The quality and orientation of the samples were controlled by X-ray diffraction and Laue backscattering patterns. X-ray phase analysis of the synthesized powder and the crushed LaB_6 single crystals was performed on a DRON-3 X-ray diffractometer in Cu K_α radiation with a Ni filter and demonstrated only reflections of the CaB_6 - type structure (sp. gr. $Pm\bar{3}m$ - O_h^1) (Fig. S4a-b). The lattice parameter of a crushed single crystal was equal 4.15720±0.00013 Å.

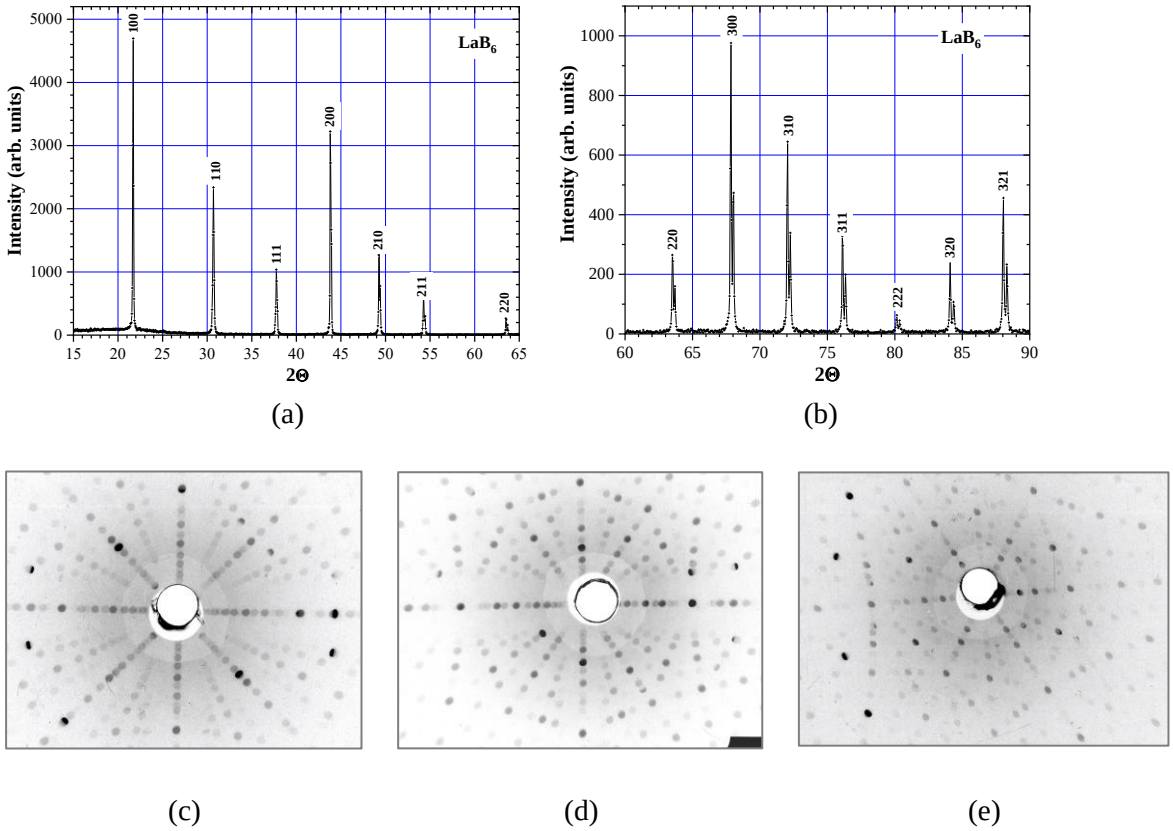

Fig. S4. **(a-b)** Typical powder X-ray diffraction pattern in Cu K_α radiation for a crushed as-grown LaB_6 crystal used for the preparation of experimental samples. X-ray Laue backscattering patterns from the oriented plates from the LaB_6 crystal # 5: **(c)** – deviation from [100] is 0.5^0, **(d)** – deviation from [110] is 2.5^0, **(e)** – deviation from [111] is 1.5^0.

Laue backscattering patterns were taken in Mo radiation both for as-grown LaB_6 crystals and oriented experimental samples prepared from them. The criterion for optimizing crystallinity was the absence of splitting of the point reflections, such as shown for the oriented plates [001], [011], [111] cut from the LaB_6 single crystal # 5 (Fig. S4c-e). These plates are used for preparation of the experimental samples, and the absence of splittings confirms the lack of domains with a misorientation more than several tenths of a degree (accuracy of the method) in the experimental samples.

The impurity composition of the grown single crystals was analyzed using an atomic emission spectrometer with inductively coupled plasma iCAP 6500 Duo (Thermo Scientific ICP, USA) with an accepted detection limit of 3 ppm. Table S4 shows the results of this analysis, taking into account all possible impurities, that are presented in the certificate for boron (the total mass fraction of the elements Na, Al, Mn, Si, Ca, Fe, Ni, Cu, Zn, Cr, Sn, Mg, Pb is not more than 0.1%) and for La_2O_3 (total mass fraction of Fe_2O_3, SiO_2, CaO, CoO, NiO, CuO, MnO_2, Cr_2O_3, CdO is no more than 0.01%). A separate column shows the maximum possible values of rare-earth elements (REE) in La_2O_3 according to its certificate. REE impurities in the LaB_6 crystals are determined by the purity of the initial La_2O_3, since zone refining process is ineffective in reducing them [2]. According to the La_2O_3 certificate, the total content of associated REE impurities did not exceed $3 \cdot 10^{-3}$ mass %. Unfortunately, the real concentration of cerium could not be determined; all emission lines had a strong background influence of the matrix (La, B). The remaining impurities present in boron and La_2O_3 are removed during synthesis and zone melting, and in the grown crystals their amount does not exceed $2 \cdot 10^{-2}$ mass %

The presence of oxygen in the grown LaB_6 single crystals was checked using pulsed reductive extraction with carbon in a flow of helium gas (the gas chromatography). The oxygen content did not exceed 0.04 mass %, i.e. oxygen is chemically bound to the surface of the crushed single crystal.

Table S4. Impurities in the LaB_6 crystals.

	# 1	**# 2**	**# 3**	**# 4**	**# 5**	**La_2O_3 certificate**
	Impurities (mass %)					
Na	0.0057	0.0020	0.0024	0.0031	0.0026	
Mg	< 0.0003	< 0.0003	< 0.0003	< 0.0003	< 0.0003	
Al	< 0.0003	< 0.0003	< 0.0003	< 0.0003	< 0.0003	
Si	0.0053	< 0.0003	0.0020	0.0057	0.0005	
Ca	< 0.0003	< 0.0003	< 0.0003	< 0.0003	< 0.0003	
Cr	< 0.0003	< 0.0003	< 0.0003	< 0.0003	< 0.0003	
Mn	< 0.0003	< 0.0003	< 0.0003	< 0.0003	< 0.0003	
Fe	0.0005	< 0.0003	< 0.0003	0.0004	< 0.0003	
Co	< 0.0003	< 0.0003	< 0.0003	< 0.0003	< 0.0003	
Ni	< 0.0003	< 0.0003	< 0.0003	< 0.0003	< 0.0003	
Cu	< 0.0003	< 0.0003	< 0.0003	< 0.0003	< 0.0003	
Zn	< 0.0003	< 0.0003	< 0.0003	< 0.0003	< 0.0003	
Zr	0.0065	< 0.0003	< 0.0003	< 0.0003	< 0.0003	
Sn	< 0.0003	< 0.0003	< 0.0003	< 0.0003	< 0.0003	
Cd	< 0.0003	< 0.0003	< 0.0003	< 0.0003	< 0.0003	
Pb	< 0.0003	< 0.0003	< 0.0003	< 0.0003	< 0.0003	
Y	< 0.0003	< 0.0003	< 0.0003	< 0.0003	< 0.0003	≤0.0005
Pr	0.0005	0.0005	0.0005	0.0005	0.0005	≤0.0005
Nd	0.0006	0.0007	0.0007	0.0006	0.0006	≤0.0005
Sm	0.0005	0.0004	0.0004	0.0007	0.0003	≤0.0005
Eu	0.0005	0.0005	0.0005	0.0005	0.0005	≤0.0005
Gd	< 0.0003	0.0006	< 0.0003	< 0.0003	< 0.0003	≤0.0005

Thus, the grown LaB_6 crystals and experimental samples prepared from them represent highly pure and structurally perfect objects for research.

[1] E.M. Dudnik, Yu.A. Kocherzhinsky, E.A. Shishkin, Yu.B. Paderno, L.I. Zadvorny, I.I. Timofeeva, L.S. Zaletilo. Investigation of the formation process of some rare-earth metal hexaborides by thermography. In: Refractory Compounds of Rare Earth Metals, Novosibirsk, Nauka, 1979, 26-29 (Russian).

[2] T. Tanaka, R. Nishitani, C. Oshima, E. Bannai, and S. Kawai. The preparation and properties of CeB_6, SmB_6, and GdB_6. J. Appl. Phys. **51** (1980) 3877-3883.
DOI: 10.1063/1.328133

[3] Y.B. Paderno, V.I. Lazorenko, A.V. Kovalev. Zone refining and growth of lanthanum hexaboride single crystals Powder Metall Met Ceram **20** (1981) 717-721.
DOI:10.1007/bf00791052

[4] Y.B. Paderno, V.I. Lazorenko, N.I. Buryak, A.V. Kovalev, A.A. Matvienko, A.P. Galasun. Amounts and character of distribution of impurities in zone-melted single-crystal lanthanum hexaboride. Powder Metall. Met. Ceram. **22** (1983) 50–53.
DOI: 10.1007/BF00792514